JOC Article

Influence of the Core Conformation on the NH-Tautomerism in Porphyrins: A Study of *meso*-(1,3-Dithian-2-yl)porphyrins

Philipp Wacker,[†] Katja Dahms,[‡] Mathias O. Senge,[‡] and Erich Kleinpeter*[,†]

Institut für Chemie, Universität Potsdam, Karl-Liebknecht-Strasse 24-25, D-14476 Golm, Germany, and School of Chemistry, SFI Tetrapyrrole Laboratory, Trinity College Dublin, Dublin 2, Ireland

kp@chem.uni-potsdam.de

Received November 14, 2007

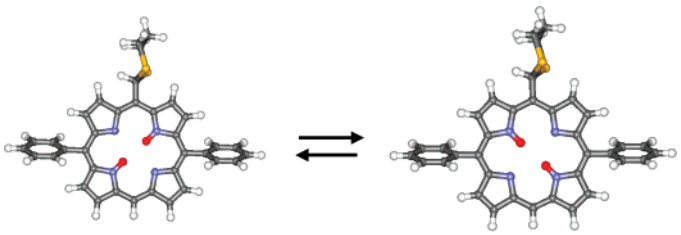

In order to investigate the mechanism of the NH-tautomerism in porphyrins, three *meso*-dithianyl-substituted porphyrins of different substitution pattern were studied theoretically. The corresponding *trans*-, *cis*- and saddle-point geometries were optimized with DFT methods, and the macrocyclic conformations obtained were analyzed using normal-structure-decomposition (NSD) analysis. Special attention was given to the influence of the participating out-of-plane and in-plane conformations on the NH-tautomerism, and the interplay of substituents, core conformations and energies of the transition-state structures was critically evaluated. The calculated energy barriers of the preferred pathways are compared with experimental activation enthalpies determined by variable-temperature (VT) NMR spectroscopy.

Introduction

The significant conformational variety of porphyrins is one reason for the manifold different physical, biological and chemical properties related to them. Therefore, porphyrins play a major role in many biological processes, for example in redox reactions and photosynthesis, and have significant application potential in industry and medicine. The importance of the porphyrin conformation for many chemical, physical and biological processes has been shown, but only few papers have addressed the relevance of the N−H groups.[1−3] The ongoing need for novel porphyrins with desired properties, which are affected by the NH-tautomerism, is critically dependent on the detailed knowledge about the inner proton-hopping mechanism and the means to fine-tune it.

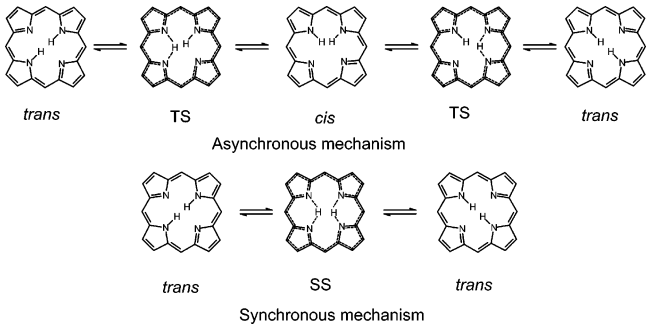

FIGURE 1. Asynchronous and synchronous mechanism of the inner proton-hopping tautomerism process of porphine.[12,14b]

Storm and Teklu were the first to explore the NH-tautomerism in porphyrins by NMR spectroscopy,[4] and significant efforts were made to elucidate the proton-exchange mechanism using NMR spectroscopy both in solution[5,6] and the solid state.[7−9]

[†] Universität Potsdam.
[‡] Trinity College Dublin.

(1) (a) Senge, M. O.; Forsyth, T. P.; Nguyen, L. T.; Smith, K. M. *Angew. Chem., Int. Ed. Engl.* **1994**, *33*, 2485−2487. (b) Senge, M. O. In *The Porphyrin Handbook*; Kadish, K. M., Smith, K. M., Guilard, R., Eds.; Academic Press: San Diego, 2000; Vol. 1, pp 239−347. (c) Senge, M. O. *Chem. Commun.* **2006**, 243−256. (d) Senge, M. O. *Acc. Chem. Res.* **2005**, *38*, 733−743. (e) Senge, M. O. *Z. Naturforsch.* **1999**, *54b*, 821−824. (f) Senge, M. O.; Kalisch, W. W. *Z. Naturforsch.* **1999**, *54b*, 943−959.

(2) Völker, S.; Macfarlane, R. M. *J. Chem. Phys.* **1980**, *73*, 4476−4482.

(3) Kasha, M. *J. Chem. Soc., Faraday Trans. 2* **1986**, *82*, 2379−2392.

(4) (a) Storm, C. B.; Teklu, Y. *J. Am. Chem. Soc.* **1972**, *94*, 1745−1747. (b) Storm, C. B.; Teklu, Y.; Sokoloski, E. A. *Ann. N. Y. Acad. Sci.* **1973**, *206*, 631−640.

(5) Abraham, R. J.; Hawkes, G. E.; Smith, K. M. *Tetrahedron Lett.* **1974**, *16*, 1483−1486.

10.1021/jo702443x CCC: $40.75
Published on Web 02/21/2008

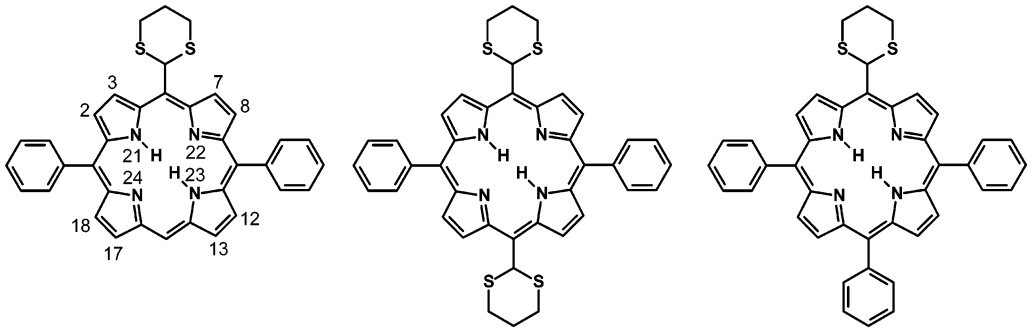

FIGURE 2. Scheme of porphyrins **1**−**3**.

To interpret the experimental results obtained for the barriers of NH-tautomerism of porphyrins, theoretical calculations were performed at different levels of theory.[10−15] Generally, both a synchronous and an asynchronous mechanism (cf. Figure 1) are discussed for the conversion of the two *trans*-tautomers into each other. In the synchronous mechanism, both inner protons jump simultaneously via a second-order saddle point, whereas in the asynchronous pathway the *trans*−*trans* conversion takes place step by step. The asynchronous inner proton-hopping mechanism in unsubstituted porphyrin (porphine) was shown to proceed via one transition state (saddle point first-order) and one *cis*-tautomer (as a local minimum) as shown in Figure 1.[11,13]

At present, the effect of the porphyrin core conformation on the NH-tautomerism is not yet clear.[16] For example, the nonplanar, *sad* distorted 2,3,7,8,12,13,17,18-octaethyl-5,10,15,20-tetraphenylporphyrin exhibits a significantly higher activation barrier than porphine while the *ruf* distorted 5,10,15,20-tetra(*tert*-butyl)porphyrin has a lower barrier.[17−19] In the latter case, the lower barrier was explained to be a result of the out-of-plane *ruffled* conformation of the porphyrin core (leading to the contraction of the porphyrin core and thereby decreasing the distance between the two inner nitrogen atoms). Maity et al. calculated a strong reduction of the N−N distance in the respective transition state of the proton-hopping process in planar porphine.[14] Ghosh found a similar distance reduction in the transition state in planar monodeprotonated porphyrin.[20] From this behavior of the parent compound it can be assumed that peripheral substituents are imposing distortion modes which further support this approach of the inner nitrogen atoms and lead thereby to decreasing the barriers to NH-tautomerism. On the other hand, it was shown previously that—strictly speaking—out-of-plane distortions do not change inner nitrogen distances.[21] Thus, the question arises, which in-plane distortions introduced by core substituents instead of the out-of-plane *ruffling* are responsible for the changes in distance?

Ogoshi et al. measured remarkably low activation energies for the tautomerism in *meso*-monosubstituted octaethylporphyrins,[22] but did not explain this unusual behavior. Ribó and coworkers showed that energetically different *cis*-tautomers exist in unsymmetrical β-substituted porphyrins. However, while structural information about the transition state could not be obtained, the most stable *cis*-tautomer should be the one in which the conformation of the bis(azafulvenic) moiety is least disturbed from planarity.[23]

The NH-tautomerism of planar porphyrins is well investigated, but less is known about the involved *cis*- and transition-state structures of the NH-tautmerism of porphyrins substituted with bulky alkyl moieties.[9−17] In this work we investigate the interplay of substitution pattern, core deformation, and preferred tautomeric pathways in a series of *meso*-dithianyl-substituted porphyrins **1**−**3** (cf. Figure 2). Special attention is given to the influence of the core conformation on the energy of the involved saddle points. In addition, the influence of the substituents on the core conformation of the tautomeric transition states is studied as well. The porphyrin core deformation of the calculated transition states is analyzed in terms of changes of bond lengths, segment planarity, and by means of the normal structure decomposition (NSD) method.

The NSD method has been developed by Shelnutt and coworkers[21] for the conformational analysis of the porphyrin core; the core conformation is decomposed into different contributions of six out-of-plane and six in-plane distortion modes: the absolute value for a distortion mode, obtained by the NSD analysis, indicates quantitatively its contribution to the overall core conformation. The NSD analysis proves to be a powerful

(6) Eaton, S. S.; Eaton, G. R. *J. Am. Chem. Soc.* **1977**, *99*, 1601−1604.
(7) Limbach, H. H.; Hennig; J.; Kendrick, R.; Yannoni, C. S. *J. Am. Chem. Soc.* **1984**, *106*, 4059−4060.
(8) (a) Frydman, L.; Olivieri, A. C.; Diaz, L. E.; Frydman, B.; Morin, F. G.; Mayne, C. L.; Grant, D. M.; Adler, A. D. *J. Am. Chem. Soc.* **1988**, *110*, 336−342. (b) Frydman, L.; Olivieri, A. C.; Diaz, L. E.; Valasinas, A.; Frydman, B. *J. Am. Chem. Soc.* **1988**, *110*, 5651−5661.
(9) Braun, J.; Schlabach, M.; Wehrle, B.; Köcher, M.; Vogel, E.; Limbach, H.-H. *J. Am. Chem. Soc.* **1994**, *116*, 6593−6604.
(10) (a) Smedarchina, Z.; Zerbetto, F. *Chem. Phys.* **1989**, *136*, 285−295. (b) Smedarchina, Z.; Zgierski, M. Z.; Siebrand, W.; Kozlowski, P. M. *J. Chem. Phys.* **1998**, *109*, 1014−1024.
(11) Reimers, J. R.; Lü, T. X.; Crossley, M. J.; Hush, N. S. *J. Am. Chem. Soc.* **1995**, *117*, 2855−2861.
(12) Boronat, M.; Ortí, E.; Viruela, P. M.; Tomás, F. *J. Mol. Struct.* **1997**, *390*, 149−156.
(13) Baker, J.; Kozlowski, P. M.; Jarzecki, A. A.; Pulay, P. *Theor. Chem. Acc.* **1997**, *97*, 59−66.
(14) (a) Maity, D. K.; Bell, R. L.; Truong, T. N. *J. Am. Chem. Soc.* **2000**, *122*, 897−906. (b) Maity, D. K.; Truong, T. N. *J. Porphyrins Phthalocyanines* **2001**, *5*, 289−299 and references therein.
(15) Cybulski, H.; Pecul, M.; Helgaker, T.; Jaszuñski, M. *J. Phys. Chem. A* **2005**, *109*, 4162−4171.
(16) Kadish, K. M., Guilard, R., Smith, K. M., Eds. *The Porphyrin Handbook*; Academic Press: San Diego, 2000; Vol. 3, p 63.
(17) Senge, M. O.; Ema, T.; Smith, K. M. *J. Chem. Soc., Chem. Commun.* **1995**, 733−734.
(18) Barkigia, K. M.; Berber, M. D.; Fajer, J.; Medforth, C. J.; Renner, M. W.; Smith, K. M. *J. Am. Chem. Soc.* **1990**, *112*, 8851−8857.
(19) Somma, M. S.; Medforth, C. J.; Nelson, N. Y.; Olmstead, M. M.; Khoury, R. G.; Smith, K. M. *Chem. Commun.* **1999**, 1221−1222.
(20) Vangberg, T.; Ghosh, A. *J. Phys. Chem. B* **1997**, *101*, 1496−1497.
(21) (a) Jentzen, W.; Song, X.-Z.; Shelnutt, J. A. *J. Phys. Chem. B* **1997**, *101*, 1684−1699. (b) Jentzen, W.; Ma, J.-G.; Shelnutt, J. A. *Biophys. J.* **1998**, *74*, 753−763.
(22) Asakawa, M.; Toi, H.; Aoyama, Y.; Ogoshi, H. *J. Org. Chem.* **1992**, *57*, 5796−5798.
(23) Garcìa-Ortega, H.; Crustas, J.; Feliz, M.; Ribò, J. M. *J. Org. Chem.* **2002**, *67*, 4170−4176.

SCHEME 1 ***trans*-Tautomers GS1 (left) and GS2 (right)**[a]

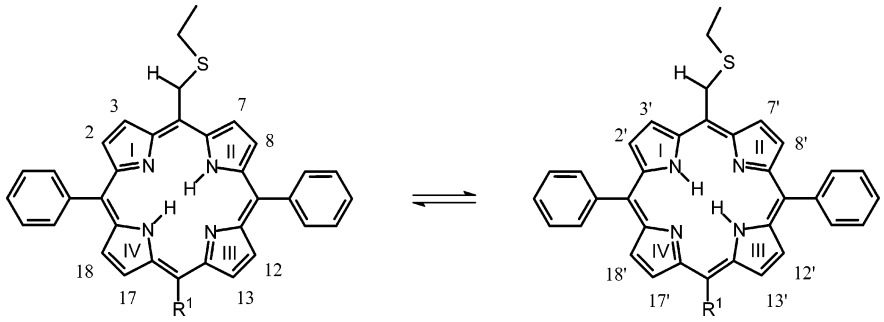

[a] The schematic side view of the dithianyl moieties illustrates their orientations. R^1: **1** = H; **2** = 1,3 dithianyl; **3** = phenyl.

tool and has been applied to the analysis of various metalloporphyrins.[24−26] Good qualitative results have also been obtained along the NSD analysis of free bases[1c,21a] and encouraged us to apply this concept for the quantitative analysis of the structures involved in the inner proton tautomerism.

As aforementioned, the conformation of an arbitrary porphyrin core can be described by the linear combination of six out-of-plane and six in-plane deformation modes, named after the symmetry of the respective distortion;[21] most common out-of-plane distortions are B_{2u} (*sad*) and B_{1u} (*ruf*). Along B_{2u} the pyrrol rings are tilted out of the mean porphyrin plane, forming a saddle-like geometry, and the meso C-atoms remain in the porphyrin general plane.[21] After B_{1u} distortion the pyrrol rings are twisted about the N−N axes, and meso C-atoms are displaced from the mean plane alternately. Both B_{2u} and B_{1u} are "soft" deformation types, and only small amounts of energy are needed for displacements along these distortion modes. For decreasing N−N distances only two in-plane distortions must be considered: B_{2g} (*m-str*) and A_{1g} (*bre*). A_{1g} describes the expanding (or contracting) of the porphyrin core, a positive contribution of A_{1g} results in gradually increase of all four N−N distances. The B_{2g} distortion will be described later in detail below for the dithianyl porphyrins studied in this contribution.

Results and Discussion

***trans*-Tautomers.** In Scheme 1 the two *trans*-tautomers of **1**−**3** are shown. Earlier,[27] we reported that, due to the orientation of the dithianyl moiety, the NH-tautomeric equilibria of **1**−**3** are shifted slightly in favor of the GS1-tautomers which are lower in energy by ca. 1.58−3.67 kJ/mol compared to the respective GS2-tautomers.

As shown in Table 1 and Figure 3, compounds **1**, **2** and **3** exhibit only very small in-plane and out-of-plane distortions.[27,28] The main difference in the conformation of the global minima structures of **1** and **3** is the slightly increased *sad* distortion of **3**; this is due to the additional phenyl group in position 15. To ascertain the role of planarity in the different segments of the porphyrin core, four segments—the respective halves of the macrocycle—were defined (I/II, II/III, III/IV and I/IV, respectively, in Scheme 1). There are no significant differences between the planarity of the different halves in the global minima structures (see also Table S1 in the Supporting Information). For porphyrin **1**, in the *meso*-dithianyl-substituted porphyrin half I/II the nonplanarity is slightly increased.

TABLE 1. NSD Analysis of Both Ground and Transition States, and Local Minima *cis*-Tautomers, of the Compounds 1−3 Studied (Complete Basis) in Å × 100

	sad B_{2u}	*ruf* B_{1u}	*m-str* B_{2g}	*bre* A_{1g}
1GS1	7.28	13.98	9.26	34.27
1GS2	1.30	11.24	9.19	34.33
1SS1	13.76	86.56	114.89	13.83
1SS2	2.10	21.78	114.26	20.98
1CISA	9.74	37.54	66.42	32.94
1CISB	5.83	1.97	58.22	34.90
1CISC	14.31	39.56	67.47	32.26
1CISD	8.78	3.42	56.93	35.01
1TSA	15.49	68.28	94.48	21.22
1TSA2	8.23	61.41	91.52	22.48
1TSB1	2.77	5.68	84.28	27.18
1TSB2	0.60	9.52	86.91	26.94
1TSC1	14.53	61.48	92.22	22.23
1TSC2	17.24	71.17	92.00	20.57
1TSD1	4.41	10.20	86.45	26.99
1TSD2	1.89	3.51	83.69	27.13
2GS1	0.01	0.01	25.67	35.90
2GS2	0.00	0.00	26.45	35.61
2SS1	23.38	161.86	95.78	17.55
2SS2	0.10	0.02	117.95	23.46
2CISA/C	15.39	99.10	53.34	22.70
2CISB/D	7.85	0.08	69.28	35.70
2TSA1/C1	25.04	138.23	74.02	9.77
2TSA2/C2	19.38	140.16	73.68	9.88
2TSB1/D1	0.04	0.13	93.08	28.60
2TSB2/D2	0.03	0.04	93.37	28.47
3GS1	11.01	10.63	14.16	35.13
3GS2	15.65	13.17	14.00	34.81
3SS1	13.45	114.65	106.22	8.71
3SS2	14.07	2.00	116.67	23.20
3CISA	5.00	48.21	55.27	32.81
3CISB	36.37	2.00	66.14	34.88
3CISC	10.14	46.72	57.54	32.26
3CISD	38.55	0.26	65.05	34.95
3TSA1	2.37	93.04	80.84	17.06
3TSA2	24.06	91.02	80.82	17.22
3TSB1	24.14	2.68	90.98	27.93
3TSB2	19.23	4.48	91.99	27.95
3TSC1	21.39	84.48	81.73	18.38
3TSC2	12.71	91.77	81.69	16.93
3TSD1	21.90	7.12	91.34	27.94
3TSD2	27.87	2.81	90.42	27.76

(24) Jentzen, W.; Unger, E.; Song, X.-Z.; Jia, S.-L.; Turowska-Tyrk, I.; Schweitzer-Stenner, R.; Dreybrodt, W.; Scheidt, W. R.; Shelnutt, J. A. *J. Phys. Chem. A* **1997**, *101*, 5789−5798.

(25) Shelnutt, J. A.; Song, X.-Z.; Ma, J.-G.; Jia, S.-L.; Jentzen, W.; Medforth, C. J. *Chem. Soc. Rev.* **1998**, *27*, 31−41.

(26) Song, X.-Z.; Jentzen, W.; Jaquinod, L.; Khoury, R. G.; Medforth, C. J.; Jia, S.-L.; Ma, J.-G.; Smith, K. M.; Shelnutt, J. A. *Inorg. Chem.* **1998**, *37*, 2117−2128.

(27) Wacker, Ph.; Dahms, K.; Senge, M. O.; Kleinpeter, E. *J. Org. Chem.* **2007**, *72*, 6224−6231.

(28) (a) Senge, M. O.; Hatscher, S. S.; Wiehe, A.; Dahms, K.; Kelling, A. *J. Am. Chem. Soc.* **2004**, *126*, 13634−13635. (b) Dahms, K.; Senge, M. O.; Bakar, M. B. *Eur. J. Org. Chem.* **2007**, 3833−3848.

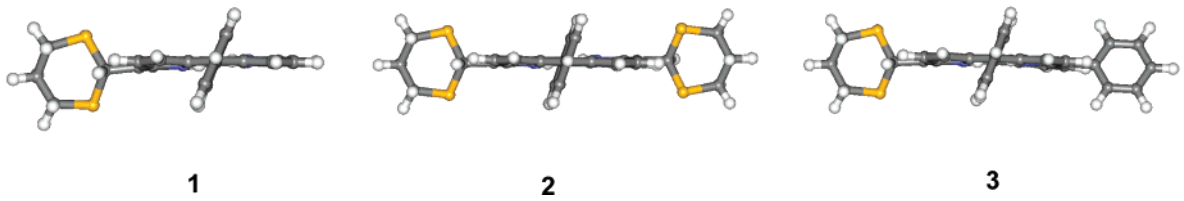

FIGURE 3. Side view of the lowest-energy structures of **1**−**3**.

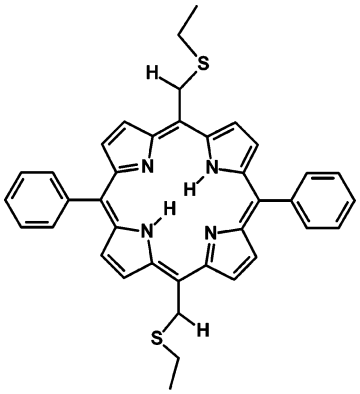

FIGURE 4. Lowest-energy tautomer of **2GS1**. The schematic side view of the dithianyl moieties illustrates their orientations.

Similarly, in compound **2** the halves I/II and III/IV are more distorted, possibly as a consequence of the alkyl substituent.

Three energetically different *trans*-tautomers were obtained for **2** in regard to the orientation of the two dithianyl groups to each other; the most stable tautomer is shown in Figure 4. All calculations regarding the inner proton-hopping mechanism are based on this structure.

Second-Order Saddle Points. In the synchronous mechanism, shown in Scheme 2, the transition states involved in the concerted movement of the inner protons are two different saddle-point structures (SS1 and SS2). The frequency analysis of SS1 and SS2 delivers two imaginary frequencies for each of the second-order saddle-point geometries. Following these modes leads to either the global minima *trans*- or the local minima *cis*-tautomers.

Generally, in all second-order saddle points the in-plane *m-str* distortion, also known as B_{2g} distortion, dominates the conformational landscape (see Table 1).[21] This in-plane distortion mode describes the stretching of the porphyrin core and results in the approach of the two adjacent nitrogen atoms sharing one hopping proton. This distortion mode was found also in a number of crystal structures of substituted porphyrins and is often referred to as "core elongation."[29] For example (cf. Table 2), in **1SS1** the distances of N21 and N24 and N22 and N23 are decreased by 0.4 Å, whereas the distances N21 and N22 and N23 and N24 increase by 0.35 Å compared to the respective *trans*-tautomers **1GS1** and **1GS2** (cf. Table 2). It is important to note that the *m-str* distortion includes an approach of the adjacent β-protons H3 and H7 in SS1 and leads, contrary to SS1, to an increase of the distance of H3 and H7 in SS2 (cf. Scheme 3).

(29) (a) Medforth, C. J.; Senge, M. O.; Forsyth, T. P.; Hobbs, J. D.; Shelnutt, J. A.; Smith, K. M. *Inorg. Chem.* **1994**, *33*, 3865−3872. (b) Senge, M. O.; Medforth, C. J.; Forsyth, T. P.; Lee, D. A.; Olmstead, M. M.; Jentzen, W.; Pandey, R. K.; Shelnutt, J. A.; Smith, K. M. *Inorg. Chem.* **1997**, *36*, 1149−1163.

SCHEME 2. Two Different Second-Order Saddle-Point Geometries SS1 and SS2 for 1−3

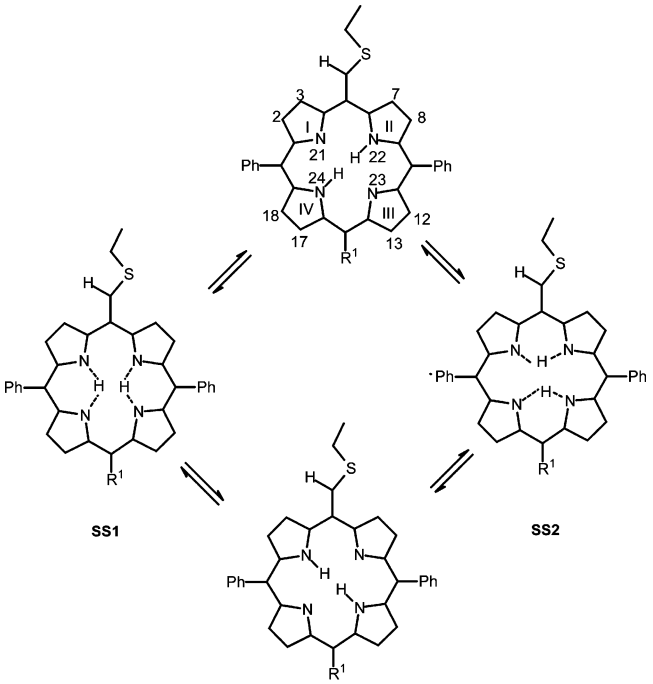

Compound	R^1
1	H
2	1,3-dithian-2-yl
3	phenyl

Consequently, steric interaction of H3 and H7 with the *meso*-dithianyl group leads to steric strain in the relevant part of the molecule. To avoid the steric strain, the porphyrin core adopts an additional *ruf* out-of-plane distortion. All SS1 species of **1**−**3** exhibit this significant *ruf* distortion which decreases in the order: **2SS1** > **3SS1** > **1SS1**. Thus, the location of both hopping protons between the pyrrole rings linked via the phenyl-substituted methine bridge results in a significantly *ruffled* core conformation as shown in Table 1 and Figure 5; the second *meso*-dithianyl group in **3** doubles the *ruf* contribution.

The geometries of all SS2 transition states reveal strong *m-str* contributions similar to those in the SS1 analogues (Table 1) decreasing in the order **2SS2** > **1SS2** > **3SS2**. A difference in the corresponding SS1 structures is the orientation of the *m-str* distortions: now the adjacent nitrogen atoms bridged by the *meso*-dithianyl group come closer, "forced" by the hopping protons. The β-protons H3 and H7 (for **2**: additionally H13 and H17), adjacent to the dithianyl group(s), move apart (cf. Scheme 3). As a result, the steric strain on the *meso*-dithianyl group is reduced to almost zero, and the porphyrin core in the SS2 transition-state structures adopts a planar conformation. In contrast to the SS1 geometries, the out-of-plane distortions in the SS2 analogues are much lower and comparable to the

TABLE 2. Interatomic Core Distances in Å of Ground and Transition States and Local Minima *cis*-Tautomers of Porphyrins 1−3

	N21H	N22H	N23H	N24H	N21N22	N22N23	N23N24	N21H24	H H
1GS1	−	1.015	−	1.015	2.958	2.904	2.985	2.914	2.201
1GS2	1.015	−	1.015		2.955	2.908	2.987	2.910	2.207
1SS1	1.293	1.293	1.293	1.293	3.307	2.462	3.330	2.460	2.530
1SS2	1.293	1.293	1.293	1.293	2.465	3.330	2.467	3.330	2.550
1CISA	1.029	1.029	−	−	3.215	2.698	3.167	2.701	2.088
1CISB	1.031			1.028	2.714	3.124	2.737	3.207	2.076
1CISC	−	−	1.032	1.031	3.143	2.694	3.242	2.697	2.131
1CISD	−	1.029	1.027	−	2.720	3.200	2.742	3.123	2.064
1TSA	1.278	1.029	−	1.341	3.258	2.645	3.245	2.494	2.345
1TSA2	1.029	1.283	1.337	−	3.259	2.496	3.248	2.646	2.346
1TSB1	1.284	1.350	−	1.028	2.511	3.215	2.683	3.259	2.332
1TSB2	1.030	−	1.348	1.292	2.657	3.226	2.516	3.265	2.344
1TSC1	--	1.338	1.281	1.031	3.226	2.494	3.287	2.644	2.371
1TSC2	1.331	−	1.031	1.284	3.221	2.641	3.281	2.492	2.368
1TSD1	−	1.029	1.294	1.347	2.661	3.260	2.517	3.227	2.340
1TSD2	1.343	1.291	1.027	−	2.511	3.254	2.686	3.215	2.329
2GS1	−	1.015	−	1.015	2.849	3.039	2.849	3.039	2.210
2GS2	1.016	−	1.016	−	2.844	3.404	2.844	3.040	2.223
2SS1	1.294	1.294	1.294	1.294	3.209	2.463	3.181	2.463	2.423
2SS2	1.293	1.293	1.293	1.293	2.463	3.351	2.463	3.351	2.564
2CISA/C	1.029	1.028	−	−	3.141	2.724	3.085	2.725	2.021
2CISB/D	1.031	−	−	1.031	2.689	3.170	2.691	3.245	2.134
2TSA1/C1	1.278	1.027	−	1.348	3.152	2.660	3.143	2.503	2.255
2TSA2/C2	−	1.341	1.283	1.028	3.141	2.501	3.148	2.660	2.249
2TSB1/D1	1.282	1.342	−	1.030	2.500	3.255	2.646	3.292	2.373
2TSB2/D2	1.031	−	1.336	1.288	2.643	3.255	2.500	3.292	2.377
3GS1	−	1.014	−	1.014	2.885	2.991	2.892	2.996	2.201
3GS2	1.015	−	1.015	−	2.883	2.990	2.893	2.993	2.210
3SS1	1.293	1.293	1.293	1.293	3.268	2.464	3.266	2.463	2.487
2SS2	1.293	1.293	1.293	1.293	2.470	3.343	2.464	3.346	2.555
3CISA	1.028	1.028	−	−	3.184	2.733	3.113	2.732	2.046
3CISB	1.032	−	−	1.030	2.696	3.155	2.705	3.233	2.114
3CISC	−	−	1.029	1.029	3.117	2.724	3.195	2.724	2.064
3CISD	−	1.030	1.030	−	2.702	3.227	2.708	3.155	2.103
3TSA1	1.283	1.028	−	1.348	3.220	2.671	3.183	2.507	2.302
3TSA2	1.028	1.287	1.344	−	3.218	2.509	3.183	2.670	2.301
3TSB1	1.282	1.344	−	1.030	2.503	3.243	2.656	3.283	2.361
3TSB2	1.031	−	1.341	1.286	2.646	3.247	2.504	3.286	2.368
3TSC1	−	1.347	1.285	1.028	3.189	2.509	3.225	2.668	2.307
3TSC2	1.341	−	1.028	1.287	3.186	2.666	3.221	2.505	2.305
3TSD1	−	1.029	1.288	1.340	2.651	3.281	2.504	3.247	2.363
3TSD2	1.337	1.289	1.029	−	2.503	3.288	2.658	3.243	2.359

SCHEME 3. In SS1, the Induced *m-str* (B_{2g}) Distortion Results in Steric Strain between the Dithianyl Moiety and H3/H7; in Contrast, This Distance between H3 and H7 Increases in SS2

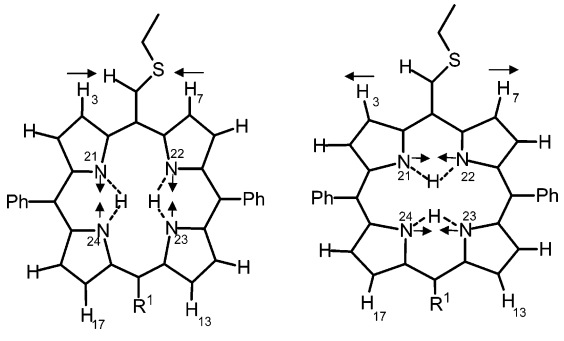

conformational distortions in the respective *trans*-tautomers. Only a minor *ruf* contribution in **1SS2** and a negligible *sad* distortion in **3SS2** were observed. In **2SS2**, out-of-plane contributions are completely absent (cf. Table 1).

With respect to the planarity of the four segments it was shown that in the *ruffled* SS1 and in the planar SS2 structures the halves including a hopping proton exhibit the lowest nonplanarity. Only in **3SS2** is the III//IV half more nonplanar than the residual halves in this transition state. This is obviously a consequence of the second dithianyl moiety (see Table S1 in the Supporting Information).

***cis*-Tautomers.** The *cis*-tautomers are characterized by both inner protons being connected to two adjacent nitrogen atoms in one-half of the molecule (cf. Scheme 4). As a consequence, and due to the different substitution pattern in compounds **1**−**3**, up to four nonequivalent and significantly different, asynchronous pathways are possible. Each of these pathways includes one *cis*-tautomer (local minimum) and two transition states (first-order saddle point). For **2**, two pathways and consequently four transition state structures exist due to symmetry reasons.

The overall dominating distortion modes for all investigated local minima *cis*-structures are the in-plane distortion modes *m-str* and *bre*. The *bre* distortion (A_{1g} distortion) describes the expansion of the porphyrin core.[21] However, compared to the *m-str* distortion the contributions of the *bre* distortion to the structures discussed are rather small (cf. Table 2).

The position of the two inner NH-protons in one-half of the molecules results in repulsive interactions which increase the distance between the corresponding nitrogen atoms. As a result, significant stretching (*m-str*) and modest expansion (*bre*) of the

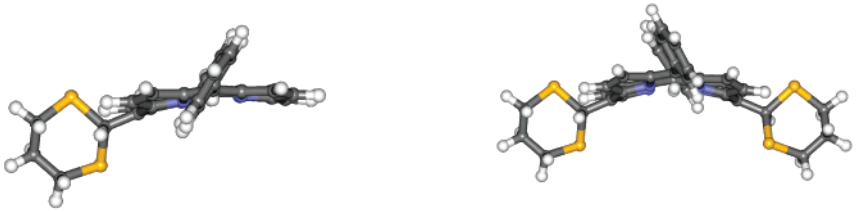

1SS1 **2SS1**

FIGURE 5. Side view of the calculated structures of **1SS1** and **2SS1**.

SCHEME 4. Representation of the Four Possible Pathways of the Asynchronous Tautomeric Mechanism[a]

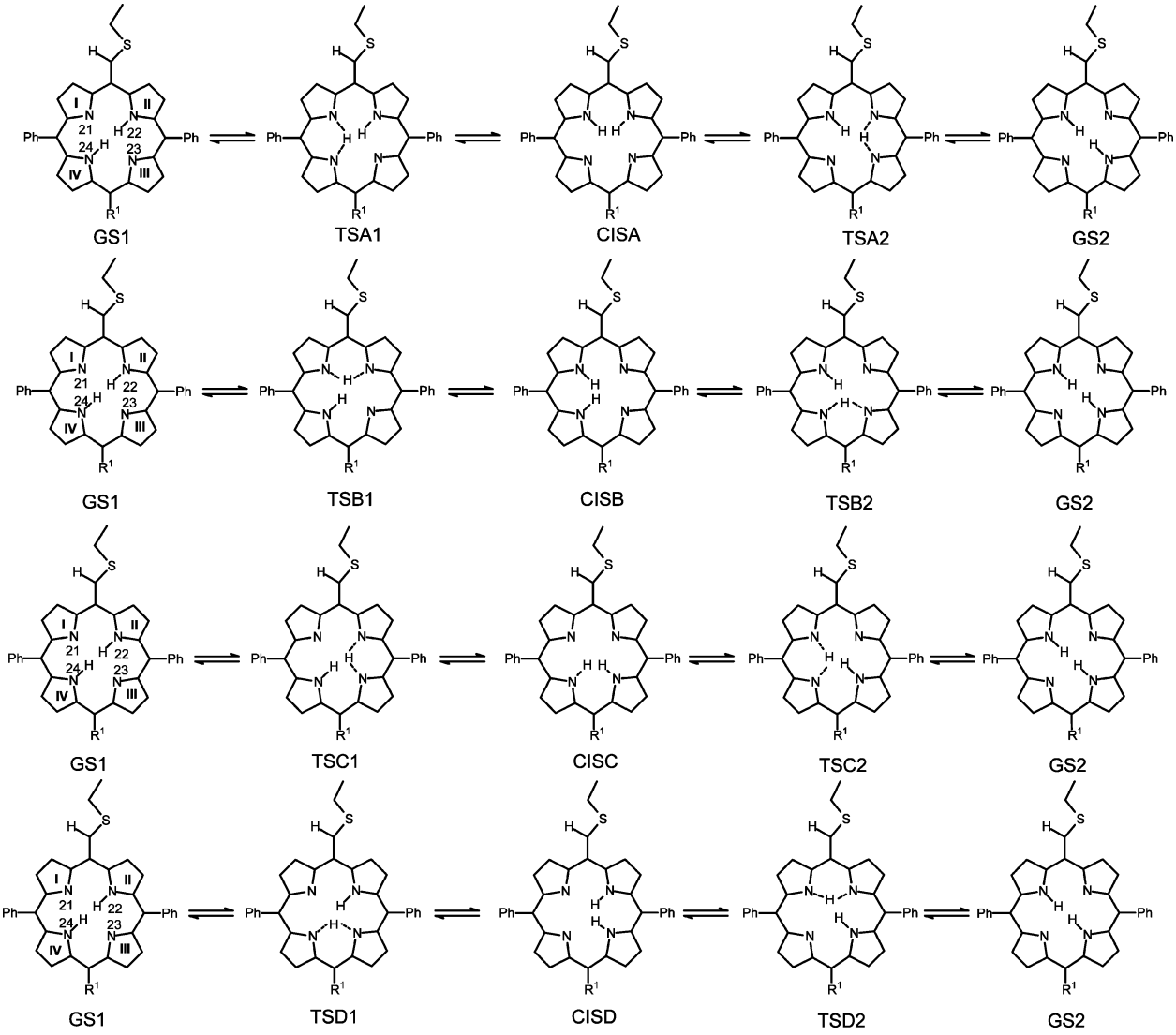

[a] The schematic side view of the dithianyl moieties illustrates their orientation. R^1: **1** = H; **2** = 1,3-dithianyl, **3** = phenyl.

porphyrin macrocycle can be observed. The degree of the *m-str* contribution is nearly the same in all *cis*-tautomers. Similar to the case described above, the *m-str* distortion results in steric strain for the *meso*-dithianyl group leading in turn to different degrees of out-of-plane distortions. In **1CISA**, **2CISA/C** and **3CISA** (cf. Scheme 4) both inner protons are bound to the adjacent nitrogen atoms belonging to the halves I/II; this segment is substituted with a *meso*-dithianyl group (see Scheme 4). The configuration leads to *ruf* distortion modes for all CISA and CISC local minima structures in the order: **2CISA/C** > **3CISA**; **3CISC** > **1CISA**; **1CISC**. In compound **2**, the *ruf* contribution is the largest for **2CISA/C**. For **2CISB/D** the out-of-plane contributions are negligible.

The degree of saddle distortion (*sad*) is modest in all *cis*-structures. As expected, the **3CISB** and **3CISD** tautomers exhibit the highest *sad* contribution. Here, additional support for the *sad* core conformation is provided by the third phenyl residue.[30,31]

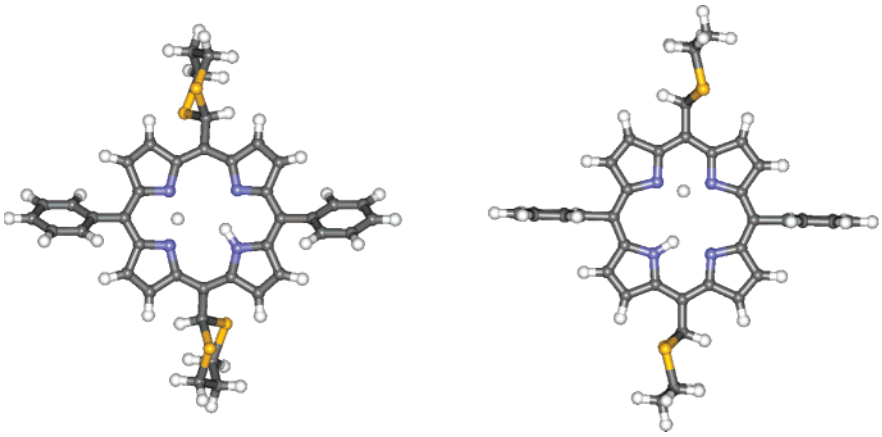

FIGURE 6. Top view of the calculated structures of **2TSA1C1** (left) and **2TSB1D1** (right).

The halves of the molecules with both inner protons (II/III and I/IV) are less distorted than the remaining halves in the **CISB** and **CISC** tautomers of **1** and **2** (cf. Table 1). However, as a consequence of the dithianyl substituent, the *meso*-dithianyl-substituted core halves in **1CISA** (I/II), **2CISA** (I/II and III/IV) and **2CISC** (I/II and III/IV) reveal the highest degree of nonplanarity. Similar results were obtained for **3**. Here, the dithianyl bearing segment I/II in **3CISA** is less planar than the remaining halves.

Transition-State Structures. As already mentioned, each asynchronous pathway includes two different transition states TS1 and TS2. All tautomeric transition state structures are characterized by two adjacent nitrogen atoms sharing the hopping proton. As a consequence, the distance between the two nitrogen atoms involved are shortened by about 0.4 Å (see Table 2). This shortening is accompanied by a *m-str* in-plane distortion which is observed for all TS-structures, too (see Table 1). Similar to the local minima *cis* structures, *m-str* distortion leads to a closer contact of the dithianyl residue and the adjacent β-protons H3 and H7 (for **2**: additionally H13 and H17). This steric strain also results in some *ruf* out-of-plane distortion (see Table 1), which is the strongest in the 5,15-dithianyl-substituted **2TSA/C** structures. In the TSB and TSD structures the β-protons adjacent to the dithianyl group diverge as a result of the *m-str* distortion and, as a consequence of the reduced steric strain, the core conformations of TSB and TSD structures exhibit only in-plane distortions and negligible out-of-plane contributions (see Figure 6).

In porphyrin **3**, with a third *meso* phenyl substituent in position 15, the transition states exhibit a minor, but constant degree of *sad* distortion. This confirms that *meso* aryl substituents support the *sad* distortion mode in the transition states in the same manner as in ground state conformations, in line with recent literature.[30,32] The N−H−N bond lengths for the hopping protons in the transition states were found to be slightly asymmetric; they are comparable to the corresponding transition states of unsubstituted porphyrin (porphine).[11,13b]

Twenty transition-state structures were calculated. In 16 of them the half of the molecule with the two nitrogen atoms sharing the hopping proton proved to be the most planar one.

TABLE 3. NH-Tautomerism: Calculated Energy Differences of SS-, *cis*- and TS-Structures, Referred to the GS1 Structure. B3LYP + ZP [B3LYP/6-31G; kJ mol^{-1}]

	synchronous pathway			asynchronous pathway		
	SS1	SS2	pathway	cis	TS1	TS2
1	64.8	76.9	A	33.1	46.4	49.4
			B	39.5	55.6	59.6
			C	35.1	49.3	50.2
			D	36.4	57.0	54.8
2	80.9	61.6	A/C	47.1	60.7	64.8
			B/D	29.5	43.9	45.6
3	77.8	65.7	A	41.2	56.8	60.5
			B	33.0	47.8	49.6
			C	41.9	59.6	60.4
			D	29.8	47.3	47.0

Strictly speaking, this is not the case in **1TSC1**, **2TSB1/D1**, **3TSB2** and **3TSD1**. However, the differences are marginal only (cf. Table S1).

Minimum Pathway. Table 3 summarizes the calculated energy differences of the SS, *cis* and TS structures with respect to the corresponding *trans*-tautomers GS1 for compounds **1**−**3**. A comparison of the energies of the second-order saddle-point structures of compound **1** reveals the ruffled form **1SS1** to be 12.1 kJ/mol lower in energy than the planar form **1SS2**. The reverse situation is found in porphyrins **2** and **3**. Here, the almost planar forms **2SS2** and **3SS2** are lower in energy compared to the ruffled structures **2SS1** and **3SS1**, respectively. Obviously, the fourth *meso* substituent changes the energetic sequence in favor of **SS2** structures, irrespective of whether it is an alkyl (**2**) or aryl (**3**) substituent.

As expected, converting an almost planar porphyrin core to an out-of-plane distorted one requires energy. The contribution of the ruffling in **2SS1** is twice as high in energy as that in **1SS1**. This is a consequence of the additional dithianyl group in **2** (Table 1). Thus, it can be assumed that converting **2GS1** to **2SS1** requires more energy than the conversion of **1GS1** into **1SS1**. Consequently, structure **2SS1** (*m-str* + *ruf*) is 19.1 kJ mol^{-1} higher in energy than the planar **2SS2** (*m-str*). While it is a well-known fact that a *meso*-phenyl group supports a *sad* core conformation, the *sad* contributions are not larger in **3SS1** and **3SS2** compared to the minima structures **3GS1** and **3GS2**. Obviously, a third *meso*-phenyl group supports the *m-str* distortion in **3SS2** to such an extent that the planar form **3SS2** (*m-str*) is 12.1 kJ mol^{-1} lower in energy than **3SS1** (*m-str* + *ruf*).

(30) Rosa, A.; Ricciardi, G.; Baerends, E. J. *J. Phys. Chem. A* **2006**, *110*, 5180−5190.
(31) Cheng, B.; Munro, O. Q.; Marques, H. M.; Scheidt, W. R. *J. Am. Chem. Soc.* **1997**, *119*, 10732−10742.
(32) Scheidt, W. R.; Lee, Y. J. *Struct. Bonding (Berlin)* **1987**, *64*, 1−70.

TABLE 4. Barriers to NH-Tautomerism, Coalescence Temperatures T_C, and Calculated Values for the Minimum Pathway

	ΔG_{exp} [kJ/mol]	T_C [K]	B3LYP [kJ/mol]	ΔB3LYP + ZP [kJ/mol]
1	48.0	250	63.0	49.4
	47.6			
2	41.5	213	60.1	45.6
	41.7			
3	45.3	231	63.6	47.3
	45.1			

The *cis*-tautomers were calculated to be 29.5−47.1 kJ mol^{-1} higher in energy than the respective GS1 *trans*-tautomers. The calculated structures **1CISA** and **1CISC**, both with significant *ruf* contributions, proved to be much lower in energy than the planar forms **1CISB** and **1CISD** (*m-str*). However, the planar structures **2CISB/D**, **3CISB** and **3CISD** (*m-str*) are lower in energy than the forms **2CISA/C**, **3CISA** and **3CISC** (*m-str* + *ruf*), respectively. As described above, an additional substituent in position 15: (i) increases the energy needed for the out-of-plane distortion and (ii) supports the *m-str* distortion resulting in the energetically favored planar tautomers **2CISB**, **2CISD**, **3CISB** and **3CISD** (*m-str*).

The calculated absolute energies show that all calculated first-order saddle points (TS) are energetically lower than the second-order saddle-point structures (SS) (cf. Table 3). Each of the possible asynchronous paths A−D includes two transition states which are energetically different. In order to convert GS1 to GS2, the transition state of highest energy for the relevant pathway is significant and must be compared with the corresponding transition states of the other pathways. The transition state of the lowest energy of these four ones thus obtained determines the preferred asynchronous pathway A−D. Following this rationale, pathway A is preferred for **1** followed by pathway C. It should be noted, that the transition states involved in pathway A exhibit the *ruf* conformation of porphyrin **1**.

For compounds **2** and **3**, the asynchronous pathways B and D are preferred. All transition states and *cis*-tautomers involved in these pathways are planar and reveal strong *m-str* contributions. Clearly, the change from the planar *trans*-tautomers **2GS1** and **2GS2** to the planar forms **2TSB/D 1** and **2TSB/D** via *m-str* distortion requires less energy than the change to the ruffled structures **2TSA1/C1** and **2TSC2/C2**. This can be understood by considering that the two dithianyl groups move the adjacent β-protons apart and thereby support the *m-str* distortion in both planar transition states easily. In addition, the fourth meso substituent supports the *m-str* distortion via additional steric repulsion on protons H13 and H17, leading to the energetic preference of the *m-str* distorted structures.

At first glance, the calculated transition-state energies with respect to the corresponding ground states agree well with the experimentally obtained data (cf. Table 4). It is known, however, that in these kinds of reactions, thermally induced tunneling contributes to proton transfers in porphyrins in both the synchronous and the asynchronous mechanism.[9,14a,33−35] Therefore, conclusions about the preferred (synchronous or the asynchronous) mechanism of the NH-tautomerism cannot be drawn easily because the partition of tunneling processes was not considered in this study. What can be concluded for sure is that the relative experimental and calculated barriers to NH-tautomerism of the studied substituted porphyrins **1**−**3** are obviously in good qualitative agreement: porphyrins **1** and **3** exhibit similar barriers to the tautomerism, whereas the corresponding barrier of porphyrin **2** reveals the lowest one, both in the synchronous and in the asynchronous mechanism (cf. Table 3). Therefore, the substituent influence in **1**−**3** on the conformation of the porphyrin core in both ground and transition states of NH-tautomerism as calculated are corroborated by the experimental values obtained by dynamic NMR spectroscopy.

It is interesting to note, that the lowest-energy pathway also includes the lowest-energy *cis*-tautomer. Thus, similar rules regarding the conformational behavior of the core can obviously be applied for the TS- and the *cis*-structures as well.

Conclusions

Both ground and transition states of NH-tautomerism of three substituted porphyrins were studied by DFT calculations at the B3LYP level of theory. Dependent on substitution for the synchronous pathway, two saddle points (SS) of significantly different energy were calculated; in addition, up to four different asynchronous NH-tautomerism pathways were found. The corresponding TS structures exhibited significant *m-str* distortion, which was the sole contributor in the lowest-energy TS of **2** and **3**. An additional *ruf*-contribution was found only in the lowest-energy TS structures of **1**. Obviously, the forth meso substituent in **2** and **3** supports the *m-str* distortion to such an extent that the transition states TSB/D (*m-str*) are energetically preferred compared to the TSA/C (*ruf* + *m-str*) transition states. The important role of the *m-str* distortion can also be found in the corresponding *cis*- and SS-structures. The hopping tautomeric NH-proton has some influence on the segment planarity: in nearly all SS- and TS-structures, the molecule half with the hopping proton exhibits the least distortion in contrast to the other halves within the respective porphyrin.

In a more general sense, it can be concluded that the NH-tautomerism studied shows a strong interplay between the in-plane *m-str* and the out-of-plane *ruf* distortion. In-plane stretching (*m-str*), occurring in all *cis*-, SS-, and TS-conformations of the porphyrins **1**−**3**, can lead to contributions of the *ruf* mode as well. The steric repulsion of the *meso*-dithianyl group and the adjacent β-protons, based on the *m-str* in-plane distortion, induces the ruffling of the macrocycle. Dependent on the number of *meso* substituents and the energy needed for the additional ruffling, structures revealing both *m-str* and *ruf* distortion modes can be higher or lower in energy compared to the analogues showing only in-plane *m-str* distortions. Furthermore, high contributions of the *m-str* distortion in the ground states lowers the barrier for the inner proton-hopping tautomerism: for the 5,15-dithianyl-substituted porphyrins **2** the lowest barrier was calculated and confirmed by the experimental VT-NMR measurements.

(33) (a) Limbach, H.-H.; Hennig, J.; Gerritzen, D.; Rumpel, H. *Faraday Discuss. Chem. Soc.* **1982**, *74*, 229−243. (b) Limbach, H.-H.; Hennig, J. *J. Chem. Phys.* **1979**, *71*, 3120−3124. (c) Schlabach, M.; Wehrle, B.; Rumpel, H.; Braun, J.; Scherer, G.; Limbach, H.-H. *Ber. Bunsen-Ges. Phys. Chem.* **1992**, *96*, 821−833. (d) Braun, J.; Limbach, H.-H.; Williams, P. G.; Morimoto, H.; Wemmer, D. E. *J. Am. Chem. Soc.* **1996**, *118*, 7231−7232. (e) Braun, J.; Schwesinger, R.; Williams, P. G.; Morimoto, H.; Wemmer, D. E.; Limbach, H.-H. *J. Am. Chem. Soc.* **1996**, *118*, 11101−11110. (f) Limbach, H.-H.; Lopez, J. M.; Kohen, A. *Philos. Trans. R. Soc. London, Ser. B* **2006**, *361*, 1399−1415.

(34) Butenhoff, T. J.; Moore, C. B. *J. Am. Chem. Soc.* **1988**, *110*, 8336−8341.

(35) Bell, R. P. *The Tunnel Effect in Chemistry*; Chapman and Hall: London, 1980.

Experimental Section

Materials. Compounds **1**−**3** were prepared, and NMR spectra were recorded already previously.[27,28] The free energies of activation were obtained from the evaluation of ^{1}H NMR spectra using the procedures of Shanan-Atidi and Bar-Eli, taking into account the unequal populations of the involved *trans*-tautomers.[27,36] As the ^{1}H resonances of the inner proton overlap, the corresponding β-protons were used to determine activation enthalpies for NH-tautomerism.

Computational Studies. Quantum chemical calculations have been performed on Origin2000 and a 1.7-GHz Linux-based personal computer using the *Gaussian03* software package.[37] For geometry optimization of all structures B3LYP and basis set 6-31G have been used.[38−41] The geometry optimizations of ground and transition states were performed without any symmetry restrictions and were followed by frequency calculations to verify the character of the stationary point obtained.

Normal-Coordinate Structural Decomposition. The theoretical background and development of this method have been described by Shelnutt and co-workers.[21] For calculations we used the NSD engine program, version 3.0 (http://jasheln.unm.edu/jasheln/content/nsd/NSDengine/nsd_index.htm).

Acknowledgment. The very useful comments of the reviewers are gratefully acknowledged. This work was generously supported by a Science Foundation Ireland Research Professorship Grant (SFI 04/RP1/B482).

Supporting Information Available: Kinetic data obtained from the ^{1}H NMR spectra, coordinates, complete NSD analysis and absolute energies of optimized structures. This material is available free of charge via the Internet at http://pubs.acs.org.

JO702443X

(36) Shanan-Atidi, H.; Bar-Eli, K. H. *J. Chem. Phys.* **1970**, *74*, 961−963.

(37) Frisch, M. J.; Trucks, G. W.; Schlegel, H. B.; Scuseria, G. E.; Robb, M. A.; Cheeseman, J. R.; Montgomery, J. A., Jr.; Vreven, T.; Kudin, K. N.; Burant, J. C.; Millam, J. M.; Iyengar, S. S.; Tomasi, J.; Barone, V.; Mennucci, B.; Cossi, M.; Scalmani, G.; Rega, N.; Petersson, G. A.; Nakatsuji, H.; Hada, M.; Ehara, M.; Toyota, K.; Fukuda, R.; Hasegawa, J.; Ishida, M.; Nakajima, T.; Honda, Y.; Kitao, O.; Nakai, H.; Klene, M.; Li, X.; Knox, J. E.; Hratchian, H. P.; Cross, J. B.; Bakken, V.; Adamo, C.; Jaramillo, J.; Gomperts, R.; Stratmann, R. E.; Yazyev, O.; Austin, A. J.; Cammi, R.; Pomelli, C.; Ochterski, J. W.; Ayala, P. Y.; Morokuma, K.; Voth, G. A.; Salvador, P.; Dannenberg, J. J.; Zakrzewski, V. G.; Dapprich, S.; Daniels, A. D.; Strain, M. C.; Farkas, O.; Malick, D. K.; Rabuck, A. D.; Raghavachari, K.; Foresman, J. B.; Ortiz, J. V.; Cui, Q.; Baboul, A. G.; Clifford, S.; Cioslowski, J.; Stefanov, B. B.; Liu, G.; Liashenko, A.; Piskorz, P.; Komaromi, I.; Martin, R. L.; Fox, D. J.; Keith, T.; Al-Laham, M. A.; Peng, C. Y.; Nanayakkara, A.; Challacombe, M.; Gill, P. M. W.; Johnson, B.; Chen, W.; Wong, M. W.; Gonzalez, C.; and Pople, J. A. *Gaussian 03*, Revision C.02; Gaussian, Inc.: Wallingford, CT, 2004.

(38) Becke, A. D. *J. Chem. Phys.* **1993**, *98*, 5648−5652.

(39) Lee, C.; Yang, W.; Parr, R. G. *Phys. Rev. B* **1988**, *37*, 785−789.

(40) Ditchfield, R.; Hehre, W. J.; Pople, J. A. *J. Chem. Phys.* **1971**, *54*, 724−728.

(41) Petersson, G. A.; Bennett, A.; Tensfeldt, T. G.; Al-Laham, M. A.; Shirley, W. A.; Mantzaris, J. *J. Chem. Phys.* **1988**, *89*, 2193−2218.